# Structure of the PH domain from Bruton's tyrosine kinase in complex with inositol 1,3,4,5-tetrakisphosphate

Elena Baraldi[1], Kristina Djinovic Carugo[1], Marko Hyvönen[1†], Paola Lo Surdo[1], Andrew M Riley[2], Barry VL Potter[2], Ronan O'Brien[3], John E Ladbury[3] and Matti Saraste[2*]

**Background**: The activity of Bruton's tyrosine kinase (Btk) is important for the maturation of B cells. A variety of point mutations in this enzyme result in a severe human immunodeficiency known as X-linked agammaglobulinemia (XLA). Btk contains a pleckstrin-homology (PH) domain that specifically binds phosphatidylinositol 3,4,5-trisphosphate and, hence, responds to signalling via phosphatidylinositol 3-kinase. Point mutations in the PH domain might abolish membrane binding, preventing signalling via Btk.

**Results**: We have determined the crystal structures of the wild-type PH domain and a gain-of-function mutant E41K in complex with D-*myo*-inositol 1,3,4,5-tetrakisphosphate (Ins (1,3,4,5)$P_4$). The inositol Ins (1,3,4,5)$P_4$ binds to a site that is similar to the inositol 1,4,5-trisphosphate binding site in the PH domain of phospholipase C-δ. A second Ins (1,3,4,5)$P_4$ molecule is associated with the domain of the E41K mutant, suggesting a mechanism for its constitutive interaction with membrane. The affinities of Ins (1,3,4,5)$P_4$ to the wild type ($K_d$ = 40 nM), and several XLA-causing mutants have been measured using isothermal titration calorimetry.

**Conclusions**: Our data provide an explanation for the specificity and high affinity of the interaction with phosphatidylinositol 3,4,5-trisphosphate and lead to a classification of the XLA mutations that reside in the Btk PH domain. Mis-sense mutations that do not simply destabilize the PH fold either directly affect the interaction with the phosphates of the lipid head group or change electrostatic properties of the lipid-binding site. One point mutation (Q127H) cannot be explained by these facts, suggesting that the PH domain of Btk carries an additional function such as interaction with a Gα protein.

Addresses: [1]European Molecular Biology Laboratory, Meyerhofstrasse 1, Postfach 102209, D-69012, Heidelberg, Germany, [2]Wolfson Laboratory of Medicinal Chemistry, Department of Pharmacy and Pharmacology, University of Bath, Claverton Down, Bath BA2 7AY, UK and [3]Department of Biochemistry and Molecular Biology, University College London, Gower Street, London WC1E 6BT, UK.

[†]Present address: Department of Biochemistry, University of Cambridge, 80 Tennis Court Road, Cambridge CB2 1GA, UK.

*Corresponding author.
E-mail: Saraste@EMBL-Heidelberg.de

Key words: crystal structure, human, immunodeficiency, inositol phosphates, PH domain, tyrosine kinase

Received: 11 November 1998
Revisions requested: 4 January 1999
Revisions received: 18 January 1999
Accepted: 28 January 1999

Published: 1 April 1999

Structure April 1999, 7:449–460
http://biomednet.com/elecref/0969212600700449

 ISSN 0969-2126

## Introduction

Non-receptor tyrosine kinases are key regulators of the growth and differentiation of hematopoietic cells [1,2]. Mutations in the gene coding for Bruton's tyrosine kinase (Btk) cause a severe hereditary immunodeficiency characterized by a block in the differentiation of pre-B-cells in bone marrow [3–5]. This results in deficiency of B cells and immunoglobulins and subsequently leads to susceptibility to infectious diseases in X-linked agammaglobulinemia (XLA) patients [6]. A similar but milder immunodeficiency, the X chromosome linked immunodeficiency (*xid*), is caused by a mutation in the murine Btk gene [7,8].

Btk is the prototype of the Tec family of tyrosine kinases [9]. In common with the kinases of the Src family, the Tec kinases contain Src-homology 3 and 2 domains (SH3 and SH2), and a catalytic SH1 domain. In addition, they contain an N-terminal pleckstrin-homology (PH) domain and a Tec-homology (TH) domain (Figure 1a), which seem to substitute for the N-terminal myristoylation site that is necessary for membrane targeting of Src. The TH domain is composed of a Btk motif adjacent to the PH domain and proline-rich region [10].

Tec kinases are involved in a variety of signalling pathways stimulated by activation of different hematopoietic receptors. The Btk activation is specifically triggered by a variety of extracellular stimuli, including cross-linking of the B-cell antigen receptor and binding of interleukin 5 [11,12]. Upon receptor stimulation, Tec kinases are recruited to the membrane where they are phosphorylated on a tyrosine (Y551) by a Src kinase, and hence activated. Activation is completed by autophosphorylation on Y223 [13,14]. The XLA mutations in Btk map to all five domains of the kinase, suggesting that they all are necessary for correct signalling [15]. Several mis-sense mutations have been found to map to the PH domain and the Btk motif. This is the only case in which mutations within a PH domain are known to cause a disease.

**Figure 1**

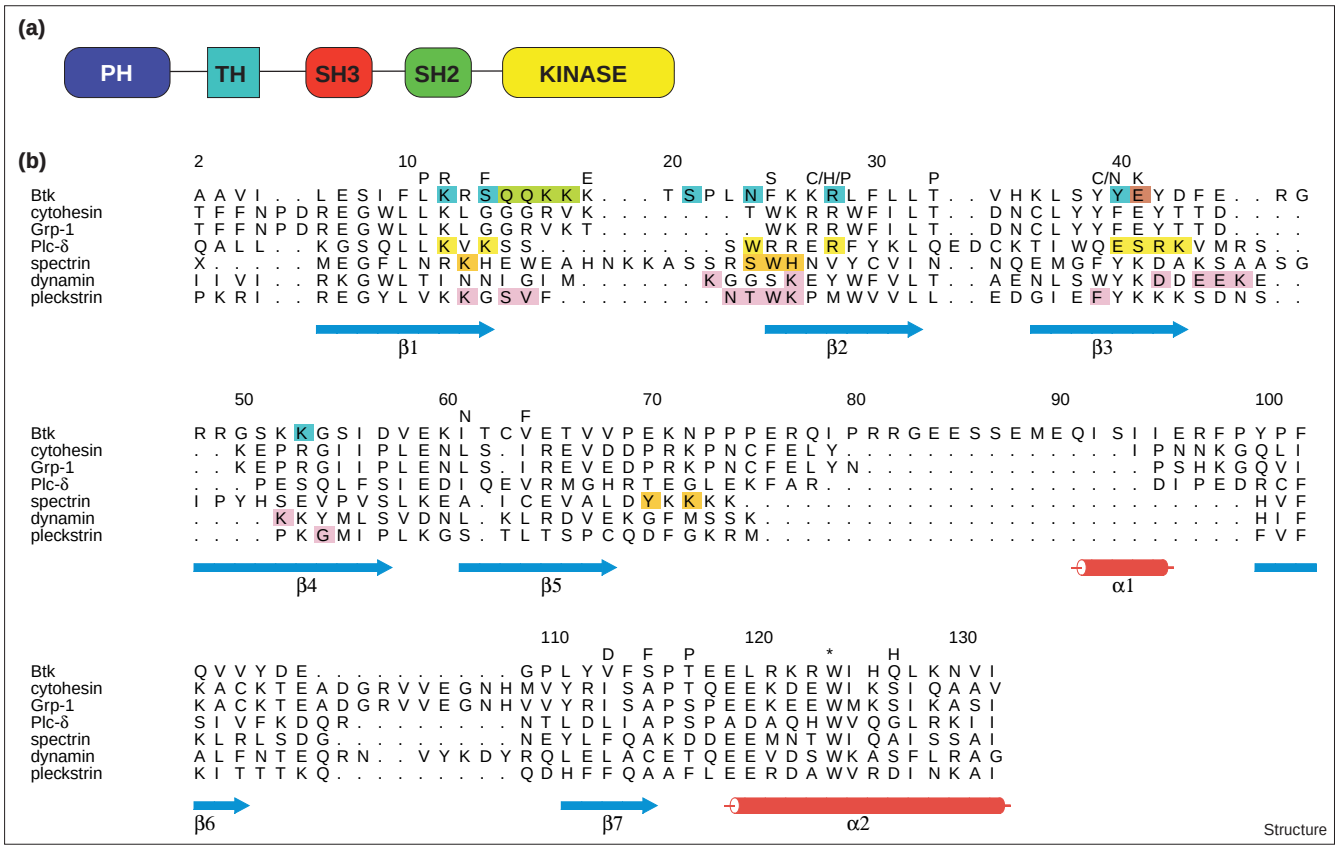


(a) Domain structure of Btk. (b) A structure-based multiple sequence alignment of PH domains. Structural alignment of PH domain from Btk, PLC-δ [31] (PDB entry 1mai), β-spectrin [38] (1btn), dynamin [28] (1dyn) and pleckstrin [27] (1pls). (The first ten NMR structures were used for the superimposition). Sequence alignment includes the PH domains of cytohesin (Genbank accession number HSU70728) and GRP-1 (Genbank MMAF1871). The secondary structure of the Btk PH domain is shown below the alignment (blue arrows for β sheets and red cylinders for α helices). The residues that are in contact with $Ins(1,3,4,5)P_4$ are coloured blue (for contacts with the sidechain) or green (for contact with the backbone atoms). The $Ins(1,4,5)P_3$-binding residues in PLC-δ and in β-spectrin are coloured yellow and orange, respectively. Residues showing chemical shifts upon $Ins(1,4,5)P_4$ interaction in dynamin and in pleckstrin are coloured pink. The residues mutated in XLA or *xid* disease are indicated above the corresponding position. The E41 residue is marked in brown. An asterisk indicates the invariant tryptophan present in PH domains. The numbering refers to the Btk PH-domain sequence.

A key regulator of the membrane recruitment of Btk is phosphoinositide 3-kinase (PI3K, [16]). PI3K phosphorylates phosphatidylinositol 4,5-bisphosphate ($PtdIns(4,5)P_2$) in the 3 position, generating phosphatidylinositol 3,4,5-trisphosphate ($PtdIns(3,4,5)P_3$) [17]. The PH domain of Btk specifically recognizes and interacts with the latter [18]. Recent data show that the SH2-containing tyrosine phosphatase SHIP, which hydrolyses $PtdIns(3,4,5)P_3$ to phosphatidylinositol 3,4-bisphosphate ($PtdIns(3,4)P_2$) [19,20], downregulates Btk activity [21], probably by decreasing its membrane-binding affinity. This underlines the important role of the PH domain in the response of Btk to regulatory stimuli.

Activation of Btk promotes growth and differentiation of B cells through a variety of downstream effectors that are not yet fully characterized. Phospholipase Cγ2, which hydrolyzes $PtdIns(4,5)P_2$ to diacyl glycerol and inositol 1,4,5-trisphosphate ($Ins(1,4,5)P_3$) [22], has been identified as a target of Btk [23,24]. The latter compound increases the intracellular calcium flux [25] by opening the $Ins(1,4,5)P_3$ receptor-gated calcium stores and, hence, generates a sustained stimulatory signal for B-cell development.

### Lipid interactions of PH domains

PH domains have low sequence similarity, but they share a common fold consisting of a seven-stranded antiparallel β sheet and a C-terminal α helix packing against it [26–28]. The PH domain of Btk has a second short α helix inserted between β strands 5 and 6 (Figure 1b). The Btk motif, a 26-residue loop that forms a binding site for a zinc ion, is essential for the structural stability of this PH domain [29]. Several PH domains have been shown to bind phospholipid head groups. They are characterized by a strong

electrostatic polarization [30], and the binding site for phosphatidylinositols is located at the positive pole [26,31]. PH domains show preferences for the binding of different phosphatidylinositols [18,32]; their binding affinities vary from the millimolar range (e.g. binding of the dynamin domain to PtdIns(4,5)$P_2$) down to the submicromolar range (as in the case of the Btk-domain binding to PtdIns(3,4,5)$P_3$ [18,33,34]). With respect to ligand specificity, they can be divided into different groups. Several domains are promiscuous and bind different inositol lipids. Some PH domains are more specific, however. For instance, the phospholipase Cδ (PLC-δ) domain is specific to PtdIns(4,5)$P_2$, the domain of AKT/PKB kinase binds to PtdIns(3,4)$P_2$ [35,36], and the Btk, GRP-1 and cytohesin domains prefer PtdIns(3,4,5)$P_3$ over other ligands [18,37].

Soluble inositol phosphates bind to the same sites in PH domains with a similar affinity to phosphatidylinositol lipids. The crystal structures of the PH domains of PLC-δ and spectrin have been determined in complex with Ins(1,4,5)$P_3$ [28,38]. Although the domains share a common fold, the ligand-binding sites involve different loops in the two proteins. However, both sites are located at the positively charged pole. The crystal structure of the *xid* mutant R28C of the Btk PH domain has been recently determined in our laboratory [29]. On the basis of this structure and XLA-mutant data, the binding site for D-*myo*-inositol 1,3,4,5-tetrakisphosphate (Ins(1,3,4,5)$P_4$) was predicted to occupy a position similar to that in PLC-δ. The Btk domain has been reported to bind to PtdIns(3,4,5)$P_3$ and Ins(1,3,4,5)$P_4$ with a $K_d$ of 800 nM and 40 nM, respectively [18,39].

The XLA-causing mutations have been divided into two main groups [29]. In one group, the mutations appear to affect the global stability of the PH domain and thus could be called 'structural mutations'. In the other group, the PH domain is properly folded, and these mutations may have a functional defect such as a decreased affinity for PtdIns(3,4,5)$P_3$; we call them 'functional mutations'. In contrast, the E41K mutant has been isolated in a random-mutagenesis study as a gain-of-function mutation [40]. Btk carrying this mutation was found to be constitutively active. This mutant can transform mouse NIH3t3 fibroblasts, and it shows enhanced tyrosine phosphorylation and enrichment to membranes in comparison with the wild-type protein [41]. This suggests that the mutated PH domain binds to membrane-bound ligands with a higher affinity than the wild type domain *in vivo*.

Here, we explore the basis for the binding specificity of Ins(1,3,4,5)$P_4$ to the Btk PH domain. Furthermore, we want to understand the effect of the functional XLA mutations within the PH domain. We have determined the crystal structures of the wild-type and E41K-mutant domains in complex with Ins(1,3,4,5)$P_4$ and also used isothermal titration calorimetry (ITC) to measure the affinity and stoichiometry of the Ins(1,3,4,5)$P_4$ binding of several XLA mutants.

## Results and discussion

### Crystal structures

The wild-type and E41K-mutant proteins containing the PH domain and the Btk motif and corresponding to residues 1–170 of human Btk were expressed in *Escherichia coli* and purified as described previously [29]. Crystals could not be obtained without the ligand. In contrast, tetragonal crystals (space group $I4_122$) grew in hanging drops after overnight incubation at room temperature when the two proteins were mixed with Ins(1,3,4,5)$P_4$ in a 1:4 molar ratio (see the Materials and methods section). Data were collected at a synchrotron facility (ESRF, Grenoble) where crystals diffracted up to 2.1 Å resolution in the case of the mutant and to 2.4 Å in the case of the wild type. The structures were determined by molecular replacement using the PH domain structure of the R28C mutant as a template (Table 1).

The Ins(1,3,4,5)$P_4$ ligand was unambiguously positioned in both E41K and wild-type domains from the analysis of their electron-density maps (Figure 2). Structures were refined to final R factors of 0.214 and 0.234 for the mutant and wild-type domains, respectively. Two molecules were found in the asymmetric unit in each structure together with 274 and 208 water molecules, respectively.

As expected, the overall structures of the unligated (R28C) domain and the wild-type and E41K domains in complex with the ligand are almost identical (Figures 3a and b). However, a striking difference is found in the position of loop β1–β2. In the R28C structure, it leans on the Btk motif, forming several polar and hydrophobic interactions. Nevertheless, it could not be properly modeled in the unligated domain because of partial disorder in the electron-density map [29]. This loop is involved in binding Ins(1,3,4,5)$P_4$ in each complex, and residues 15–23 undergo a conformational change with movements of Cα atoms ranging from 1.8 Å at position Q15 to 11.0 Å for residue T20. The ligand promotes the loop movement and stabilizes its conformation, rendering its electron density clearly visible. This structural rearrangement leads to the loss of the polar contacts between the Q16 sidechain and the mainchain and sidechain atoms of N149, and the hydrophobic interaction between the aliphatic part of the Q16 sidechain and aromatic W147. This loss of stabilizing interactions in this region of the β1–β2 loop is compensated by a number of new contacts with the ligand, as described below.

### Ins(1,3,4,5)$P_4$-binding site

The amino acids involved in the interaction with Ins(1,3,4,5)$P_4$ are located in the β1–β2 and β3–β4 loops.

**Table 1**

**Data collection and refinement statistics.**

| | Wild type | E41K |
|---|---|---|
| Resolution (Å) | 35.0–2.4 | 35.0–2.1 |
| Wavelength (Å) | 0.947 | 0.947 |
| Completeness*(%) | 96.5(97.6) | 99.4(99.5) |
| Rmerge*† | 0.044(0.346) | 0.037(0.322) |
| Number of unique reflections | 25487 | 39294 |
| Refinement statistics (TNT) | | |
| Resolution (Å) | 2.4 | 2.1 |
| R factor‡ | 0.234 | 0.214 |
| R free | 0.351 | 0.296 |
| Number of protein atoms (molecule A/molecule B) | 1362/1348 | 1376/1338 |
| Number of water molecules/zinc ions | 208/2 | 274/2 |
| Number of ligand molecules | 2 | 4 |
| Mean B of protein atoms (Å$^2$; molecule A/molecule B) | 55.3/62.5 | 34.1/44/9 |
| Mean B of solvent atoms/zinc ions (Å$^2$) | 70.4/65.2 | 50.9/42.8 |
| Mean B of ligand atoms (Å$^2$; molecule A/molecule B) | 44.62/54.34 | 28.16/34.11<br>55.4/55.6 |
| Geometrical statistics | | |
| Rmsd from ideal bond length§ (Å) | 0.022 | 0.020 |
| Rmsd from ideal bond angles§ (°) | 2.87 | 2.10 |

*Values in parentheses are for the highest shell. †$R_{merge}$= $\Sigma|I_i-\langle I\rangle|/\Sigma I_i$, where $I_i$ is the intensity of an individual reflection and <I> is the mean intensity of that reflection. ‡R factor = $\Sigma|F_o-F_c| / \Sigma F_o$. §Rmsd is root mean square deviation.

The ligand interacts with the PH domain directly, forming 18 hydrogen bonds, and indirectly via several water molecules (Figure 3c). Key residues coordinating the ligand are K12 and R28, which interact with the 3- and 4-phosphates, and the residues on the β1–β2 loop, which are involved in the interaction with the 5-phosphate. K12 contacts both 3- and 4-phosphates with two and one hydrogen bonds, respectively. Indirectly, K12 is also in contact with the OH group in the 2 position of the inositol ring via a water molecule. The sidechain of R28 contacts the 3-phosphate with two hydrogen bonds. These interactions completely bury the 3- and 4-phosphates in a cavity formed by loops β1–β2 and β3–β4. In addition, the 4-phosphate directly interacts with the sidechain of Y39 and the backbone NH group of Q15, and, via two water molecules, with the backbone carbonyl group of K53 and the sidechain of K17. The 3-phosphate contacts the sidechain of K53 of strand β4 via a water molecule (Figure 3c).

**Figure 2**

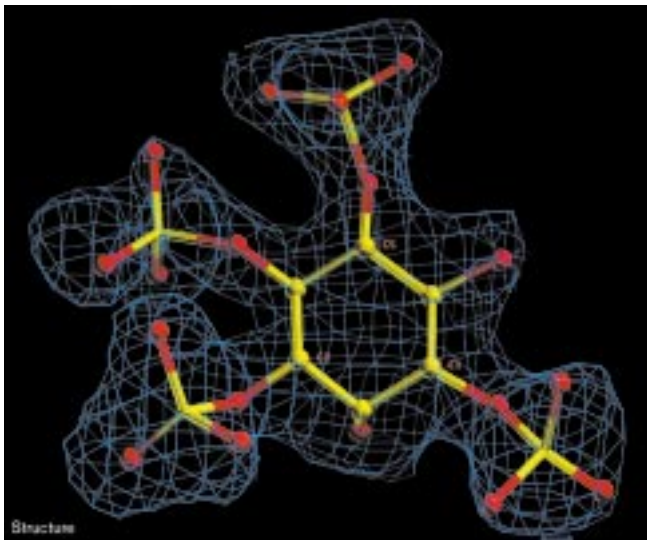

The $F_o$–$F_c$ electron-density map of Ins(1,3,4,5)$P_4$ bound to the PH domain of the E41K mutant (chain A), contoured at 3σ. A similar density is found for the ligand bound to the wild-type domain in the corresponding position.

Residues 16–18 in the β1–β2 loop contact and stabilize the 5-phosphate. The backbone NH groups of these residues interact with this phosphate via several hydrogen bonds. Apart from the sidechain of K18, which also contacts the 5-phosphate, the sidechains of these residues are exposed to the solvent and point away from the binding site. The 5-phosphate also interacts with the sidechain of S21. The 1-phosphate, which forms the link to the rest of the phospholipid structure in PtdIns(3,4,5)$P_3$, points away from the binding site and interacts with the sidechains of N24 and K26, and with water molecules. These water molecules bridge the 1- and 3-phosphates to the sidechains of K53 and K18. Finally, the OH group in the 6 position of the inositol ring is within hydrogen-bonding distance of the

**Figure 3**

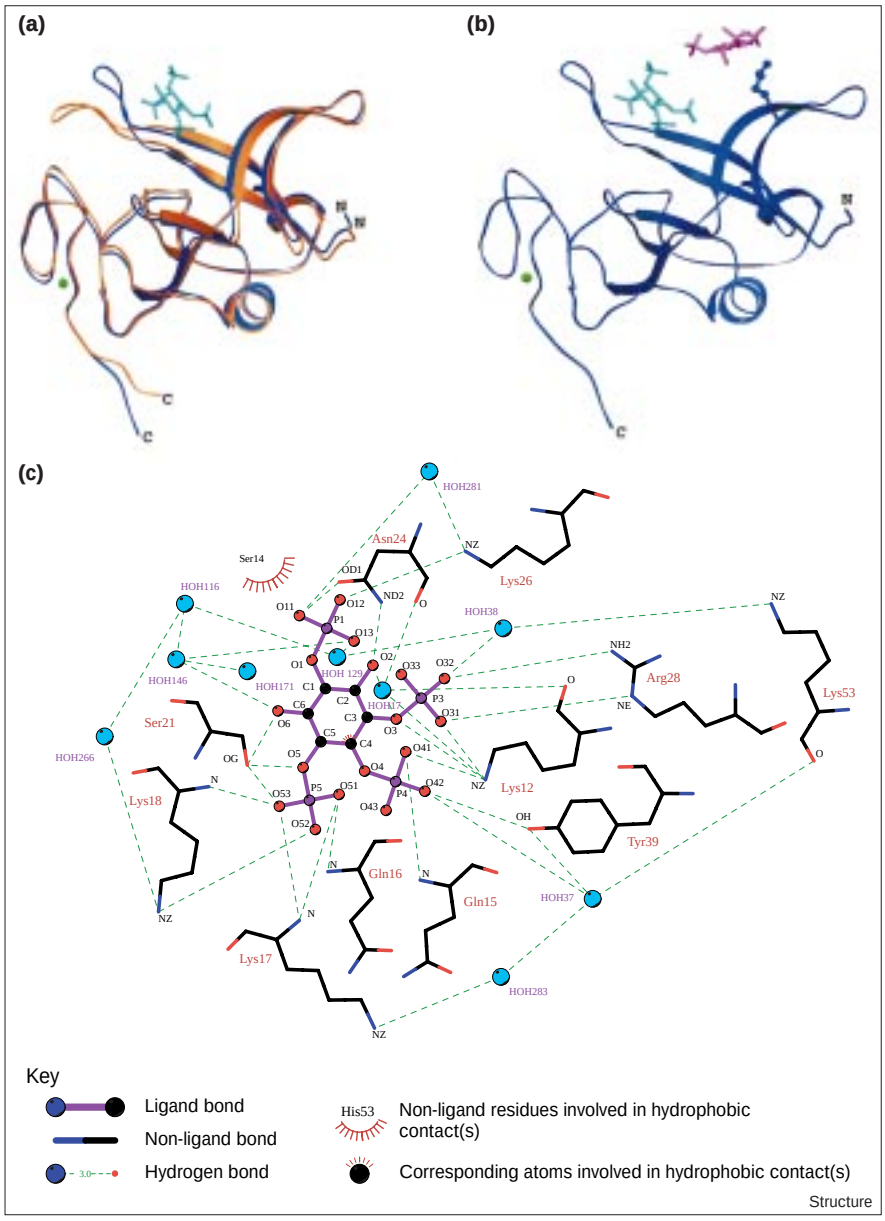


(a) Comparison between the unligated Btk PH-domain (R28C) structure, in orange, and the wild-type domain bound to Ins(1,3,4,5)$P_4$ in blue. The two structures were superimposed by the program ALIGN [67]. Ins(1,3,4,5)$P_4$ is in cyan and the bound zinc ions in the Btk motif are in green. (b) The E41K PH domain in complex with two molecules of Ins(1,3,4,5)$P_4$. The second Ins(1,3,4,5)$P_4$ molecule (pink) is bound adjacent to the E41K mutation. Ins(1,3,4,5)$P_4$ is in cyan and the zinc ion is in green. The figure was prepared with the program SETOR [68]. (c) Plot of the interactions between the PH domain and Ins(1,3,4,5)$P_4$ drawn with the program LIGPLOT [69]. The E41K (chain A) was chosen for the calculation because of its higher resolution, but similar interactions are seen in the wild-type domain. Only distances below 3.5 Å are indicated (the distances will be available at http://www.embl-heidelberg.de/ExternalInfo/Saraste/projects.html).

sidechain of S21, and the OH group in the 2 position is hydrogen-bonded to the sidechain of N24, and the inositol ring interacts via hydrophobic contacts with the sidechain of S14 (Figure 3c).

Three elements, the sidechains of K12 and R28 on one side, and the backbone NH group on the β1–β2 loop on the other side, already provide a sufficiently high number of contacts for positioning the 3-, 4- and 5-phosphates in a stable interaction, which accounts for the high affinity and specificity of the Btk PH domain for Ins(1,3,4,5)$P_4$ over Ins(1,4,5)$P_3$. In competition experiments *in vitro*, the $K_d$ for the binding of the Btk domain to Ins(1,3,4,5)$P_4$ has been calculated to be 15 nM, whereas the $K_d$s for Ins(1,4,5)$P_3$ and inositol 1,3,4-trisphosphate (Ins(1,3,4)$P_3$) have been estimated to be in the micromolar range (54 and 11 μM, respectively [42]). The crystal structure indicates that the absence of a third phosphate group would deprive this interaction of a significant number of hydrogen bonds; this would explain the dramatic decrease in the affinity. The structure also indicates that a phosphate in the 2 position would sterically interfere with binding, whereas a 6-phosphate could be accommodated. The binding experiments are consistent with this, indicating that the $K_d$ for the D-*myo*-inositol 1,3,4,5,6-pentakisphosphate (Ins(1,3,4,5,6)$P_5$) complex is approximately 90 nM [42].

**Figure 4**

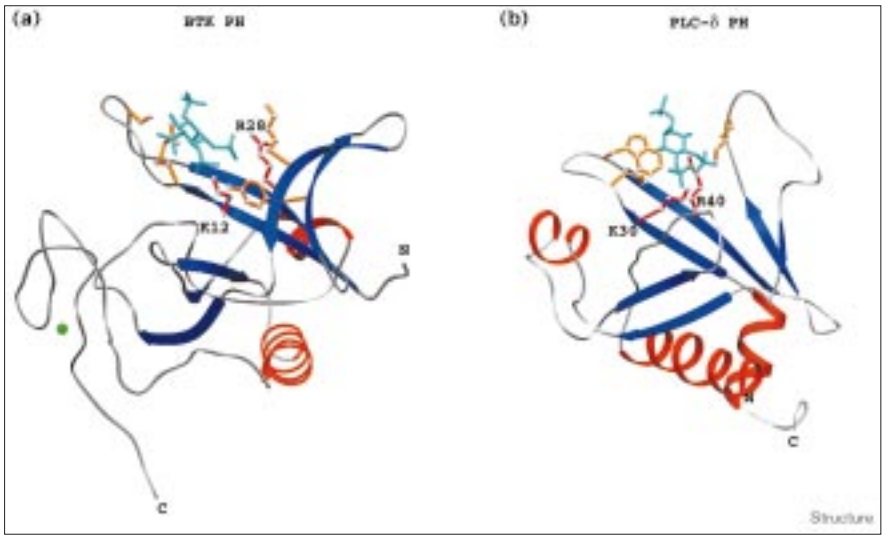


Comparison between the inositol phoshate binding sites in the (a) Btk PH domain and (b) in the PLC-δ PH domain [31]. Only the residues that are most important for the interaction are indicated and coloured red and orange. K12 and R28 in Btk superimpose with K30 and R40 in PLC-δ. The $Ins(1,3,4,5)P_4$ in Btk and the $Ins(1,4,5)P_3$ in PLC-δ are in cyan.

### Comparison with inositol phosphate binding sites in other PH domains

Seven different PH-domain structures have been determined by X-ray crystallography and/or nuclear magnetic resonance (NMR) spectroscopy [26–29,31,38,43–46], but only two have been solved in complex with an inositol-phosphate ligand. The latter are the PLC-δ PH domain [31], which binds $Ins(1,4,5)P_3$ with a $K_d$ of 210 nM, and the β-spectrin PH domain [38], which binds the same ligand with a much weaker affinity ($K_d$ = 40 μM). $Ins(1,4,5)P_3$ binds to these two domains in distinct sites, which consist of the β1–β2 and β1–β2 loops in the case of the β-spectrin domain, and β1–β2 and β3/β4 loops in the case of the PLC-δ domain.

As expected [29], the binding site in the Btk domain has the same location as in the PLC-δ domain, namely between the β1–β2 and β3–β4 loops. Furthermore, the sidechains of K12 and R28 in the Btk domain superimpose with K30 and R40 of the PLC-δ domains, which contact the 4- and 5-phosphates of $Ins(1,4,5)P_3$ in the latter [31] (Figure 4). These two residues are also conserved in GRP-1 and cytohesin PH domains (Figure 1b), which, similar to the Btk domain, bind with a higher specificity to $PtdIns(3,4,5)P_3$ than to $PtdIns(4,5)P_2$ [37].

Interestingly, the inositol ring in the PLC-δ complex is in a position that is symmetrical to the one adopted in the Btk complex (Figure 4). The $Ins(1,3,4,5)P_4$ ligand of the latter is rotated by 180° around the axis defined by the line connecting the 1- and 4-phosphates in comparison with the $Ins(1,4,5)P_3$ bound to the PLC-δ PH domain. Hence, the 3-phosphate in the Btk complex superimposes with the 5-phosphate of the PLC-δ complex, and together with 4-phosphate, is buried inside the interior of the binding pocket. The crystal structure indicates that the phosphate that chiefly accounts for the higher affinity of the Btk complex with respect to the PLC-δ one is not the 3-phosphate but rather the 5-phosphate, which makes a number of contacts with the backbone of the β1–β2 loop. This loop is six residues shorter in the PLC-δ domain (Figure 1b) and provides less stabilizing contacts to the $Ins(1,4,5)P_3$ ligand, leaving the 2 and 3 positions of the inositol ring solvent-exposed. In the PLC-δ PH domain, the inositol ring makes a hydrophobic contact with the sidechain of W36. The sidechain of N24 in the Btk domain, which aligns with W36 (Figure 1b), contacts the ligand with hydrogen bonds. A hydrophobic contact with the inositol ring is made by the sidechain of S14 in the Btk complex (Figure 3c).

The sidechains of K17, K18 and K19 in the loop β1–β2 are solvent-exposed and do not take part in the binding. Positive residues are also found in the corresponding sequences of GRP-1 and cytohesin PH domains (Figure 1b). This suggests an important role for these residues in building a positively charged array necessary for the correct orientation and anchoring of the PH domain on negatively charged membranes.

### The E41K mutant

The $Ins(1,3,4,5)P_4$-binding site in the E41K and wild-type complexes is identical (Figure 3). The mutated residue is located in the strand β3. This mutation, which replaces a negative charge with a positive one, is responsible for the constitutive membrane association and activation of Btk [40], suggesting that the K41 residue would provide more contacts with the bound $Ins(1,3,4,5)P_4$ [29]. However, the sidechain of K41 points away from the domain core and is not in contact with the bound ligand (Figure 3b). Comparison between the electron-density maps of the

**Figure 5**

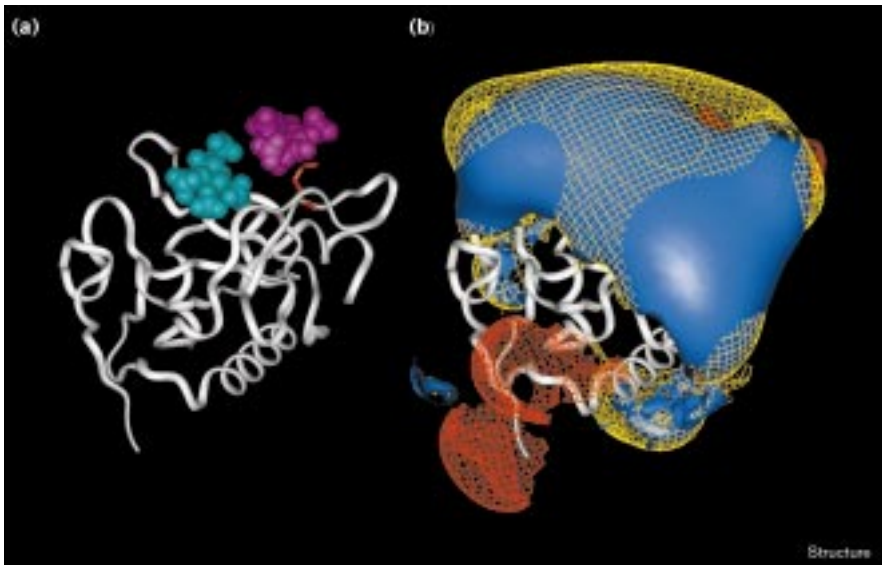


The polarized electrostatic potential contoured at +0.6 kT (solid blue and net yellow) and –0.6 kT (orange). In (a), the backbone of the domain with the E41K mutation and the two ligands are shown (the second Ins(1,3,4,5)$P_4$ molecule is coloured purple). In (b), the positive electrostatic potential of the wild-type domain (solid blue) and the E41K PH domain (net yellow), both calculated without ligand, are superimposed. The arrow indicates the position of the E41K mutation. The figure was prepared with the program INSIGHT II [70].

mutant and wild-type PH domains revealed that a second Ins(1,3,4,5)$P_4$ molecule is bound to K41. The second Ins(1,3,4,5)$P_4$ is located on the crystallographic twofold axis and is sandwiched between two symmetry-related PH molecules that face each other in the crystal packing (see the Materials and methods section). Unlike the other ligand, it is not accommodated in a pocket, but it is in a more exposed position and only makes contacts with the sidechains of K26, K41 and K53. Its electron-density map is more disordered in comparison with the map of the first Ins(1,3,4,5)$P_4$ in the pocket.

Comparison between the electrostatic potential of the wild-type and the E41K mutant (Figure 5) reveals that this mutation enlarges the positively charged surface in a region located above β strands 3 and 4, where the second Ins(1,3,4,5)$P_4$ binds in the crystal. It is likely that other negatively charged inositol phosphates, such as Ins(1,4,5)$P_3$, could be accommodated in this position to neutralize the positive charge of K41. Therefore, this second interaction may lack proper specificity and can be explained by the increase in the local electrostatic potential.

### Analysis of XLA mutations

The XLA mutations, which map to the PH domain and the Btk motif [15] are shown in Figure 6. Structural mutations occur in positions that are considered crucial for the folding and stability of the domain. We have previously classified mutations L11P, F25S, T33P, V64F, V113D and C155G/R in this category [29]. During the course of this study, new XLA mutations K19E, Y40C, I61N, S115F, T117P, Q127H and C154S in the PH domain and Btk motif have been added to the Btkbase (Figure 6). Y40 and I61 are in the hydrophobic core of the PH domain. Their substitution with cysteine and asparagine, respectively, would result in structural instability. T117P and C154S can also be classified as structural mutations. T117 is found at the beginning of the C-terminal α-helix. A proline in this position would disrupt the structure of this α helix, which packs against the β sheet and stabilizes the global fold. We have expressed the T117P mutant and found that the protein is not soluble. C154 coordinates the zinc ion, which is crucial for the conformation of the loop corresponding to the Btk motif [29]. Mutations in this position would unfold the Btk motif, destabilizing the PH domain as well.

The rest of the mutations are predicted to impair the functional properties of the PH domain without affecting the core structure (Figure 6). Among these, the three mutations of R28 are likely to perturb the interaction with inositol phosphates. This residue is in contact with the 3-phosphate of Ins(1,3,4,5)$P_4$. All three mutations (R28C, R28H and R28P) would remove the positive charge and would not provide sidechains suitable for binding to the 3-phosphate. Accordingly, the R28C and R28H mutants have been found to bind to Ins(1,3,4,5)$P_4$ with greatly reduced affinity [39]. The K12 sidechain lies in the middle of the binding pocket contacting the 3- and 4-phosphates. The longer sidechains of the K12R and S14F mutants would clash against the ligand and sterically hinder its binding.

Interestingly, K19E and Q127H could both be functional mutations (Figure 6). Each protein can be expressed in a soluble form in *E. coli*. However, each residue is exposed to the solvent and neither one is in contact with the Ins(1,3,4,5)$P_4$ molecule. K19 is located in the β1–β2 loop but its sidechain points away from the bound ligand. Its position mirrors the position of the lysine in the E41K

**Figure 6**

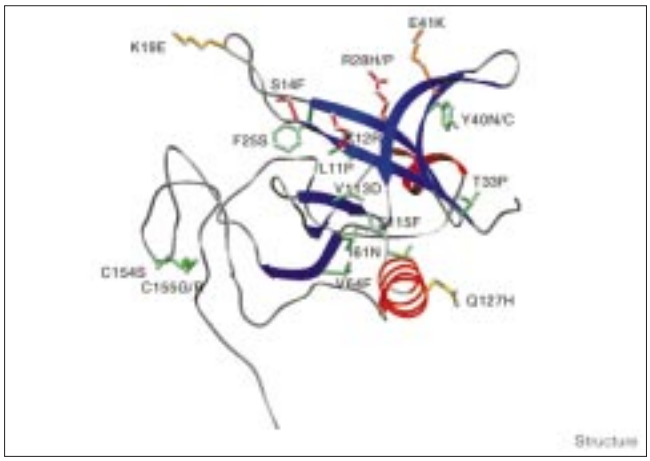


The point mutations causing the XLA or *xid* phenotype are shown. The residues that are in contact with Ins(1,3,4,5)$P_4$ and classified as functional mutations are coloured red. Those residues that are not in contact with Ins(1,3,4,5)$P_4$, but are still classified as functional mutations, are coloured yellow. Structural mutations are coloured green. The E41K mutation is coloured orange. For a list of the current XLA mutations [71] affecting the PH domain and Btk motif see http://www.uta.fi/imt/bioinfo/BTKbase/. The two functional mutations that are not in contact with the Ins(1,3,4,5)$P_4$ ligand are shown in bold. Folding mutants are L11P, F25S, T33P, Y40C/N, I61N, V64F, V113D, S115F, T117P, C154S and C155G/R. Functional mutants are: K12R, S14F, K19E, R28H, R28P, R28C (*xid*) and Q127H.

**Figure 7**

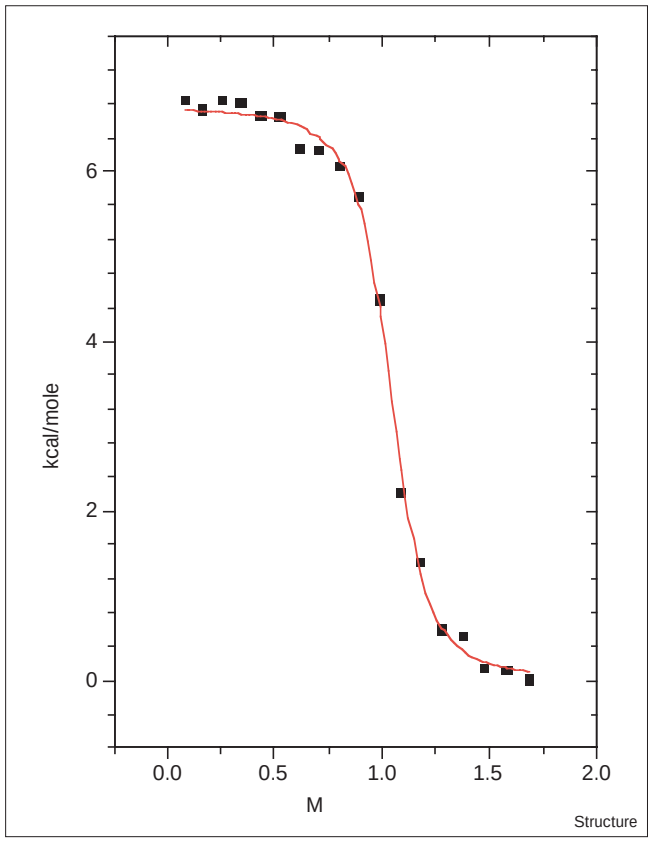


A typical isothermal titration for the interaction of Ins(1,3,4,5)$P_4$ with Btk mutant Q127H. The points correspond to the enthalpy per molar ratio (Ins(1,3,4,5)$P_4$/protein), and the data have been fitted with a nonlinear least-squares algorithm, giving $K_B = 1.26 \times 10^7\ M^{-1}$, $\Delta H$ = + 6.8 Kcal $mol^{-1}$, and stoichiometry = 1.01 (Table 2).

mutant, which is located on the opposite side of the binding site in the β3–β4 loop (Figure 6). The E41K mutation increases positive electrostatic potential at this end of the domain, whereas the K19E mutation has an opposite effect and consequently may decrease the affinity for the negatively charged membrane surface.

We cannot explain the effect of Q127H substitution in terms of perturbation of inositol-phosphate binding or the electrostatic polarization. This residue is in the C-terminal α helix, which is located on the opposite side of the Ins(1,3,4,5)$P_4$-binding pocket, and its sidechain is solvent-exposed (Figure 6). It is tempting to think that this XLA-causing mutation reflects a functional property of the PH domain that is not related to phospholipid binding. It has been proposed that some PH domains bind to the $G_{\beta\gamma}$-subunit complex of heterotrimeric G proteins [47]. Experimental data indicate that the Btk PH domain may also bind to the $G_{\beta\gamma}$ complex in a manner similar to that of the PH domain of β-adrenergic receptor kinase [48]. In addition, it has been reported that the $G_\alpha$ subunit can stimulate Btk activity [49]. The residues involved in binding to $G_\alpha 12$ have been mapped to the C terminus of the PH domain and to the Btk motif [50]. The Q127 residue is located in this area, and the Q127H mutation could abolish such an interaction.

### Binding affinities

We have expressed and purified several PH-domain mutants to study their binding affinities to Ins(1,3,4,5)$P_4$ by ITC [51]. According to the structural analysis, the loss-of-function mutations K19E and Q127H, and the gain-of-function mutation E41K should not alter binding affinity to Ins(1,3,4,5)$P_4$. The experimental data (Table 2 and Figure 7) show that the wild type, Q127, K19E and E41K bind to Ins(1,3,4,5)$P_4$ with a similar affinity.

The three mutants have an affinity in the range of 80–90 nM, which is only twofold lower than the affinity of the wild-type domain (40 nM, Table 2). Conversely, the binding isotherms of the functional mutants K12R and R28C, which are predicted to affect the ligand binding, were similar to the heat of dilution, indicating that no detectable interaction takes place.

Under the conditions employed for the binding experiments, the interaction between the Btk PH domain and Ins(1,3,4,5)$P_4$ is entropically driven, as it has a favorable

**Table 2**

**Titration calorimetry of the Ins(1,3,4,5)$P_4$ binding to the Btk PH domains.**

| PH domain | Stoichiometry *n* | $K_B$ ($10^7$ $M^{-1}$) | $K_D$ nM | ΔG° kcal/mol | ΔH kcal/mol | TΔS° kcal/mol |
|---|---|---|---|---|---|---|
| wild type | 1.0 ± 0.4 | 2.49 ± 0.63 | 40 | –9.80 | +6.7 ± 0.1 | +16.5 |
| E41K | 1.0 ± 0.4 | 1.14 ± 0.37 | 87 | –9.33 | +6.4 ± 0.1 | +15.7 |
| K19E | 1.0 ± 0.4 | 1.09 ± 0.55 | 92 | –9.28 | +3.6 ± 0.2 | +13.0 |
| Q127H | 1.0 ± 0.4 | 1.26 ± 0.16 | 79 | –9.36 | +6.8 ± 0.1 | +16.2 |

The values of stoichiometry *n*, binding constant $K_B$, dissociation constant $K_D$, free energy ΔG°, heat of interaction ΔH and entropy TΔS° measured by ITC for different PH domains at 15°C.

entropic and a very small enthalpic contribution to the free energy (Table 2). The entropic effect is likely to be attributed to the release of water molecules from the binding site upon ligand interaction. The calculated stoichiometry of the binding of the wild-type domain and the K19R, E41K and Q127 mutants is equal to 1. This indicates that the binding affinity of the second Ins(1,3,4,5)$P_4$ that is present in the crystal structure of the E41K mutant is too low to be detected in solution, and it further supports the unspecific character of the interaction with the second ligand.

### Classification of the XLA mutants

Our data suggest that four kinds of mutants can been identified. Structural mutations perturb the stability of the PH-domain core or abolish binding of zinc to the adjacent Btk motif. The bulk of the functional mutations weaken binding of the PtdIns(3,4,5)$P_3$ head group in a specific binding site. The K19E mutation has an effect on the electrostatic potential in the region surrounding the phosphatidylinositol-binding site. The reversal of an electric charge in this region (E41K) can cause a gain of function. Finally, none of the explanations above fits to the Q127H mutation, which is predicted to perturb a different function such as the interaction with $G_\alpha 12$.

### Dimerization of the PH domain and interaction with membrane

Phosphatidylinositols phosphorylated in the 3 position, such as PtdIns(3,4)$P_2$ and PtdIns(3,4,5)$P_3$, are not normally present in the membranes of quiescent cells but they are

**Figure 8**

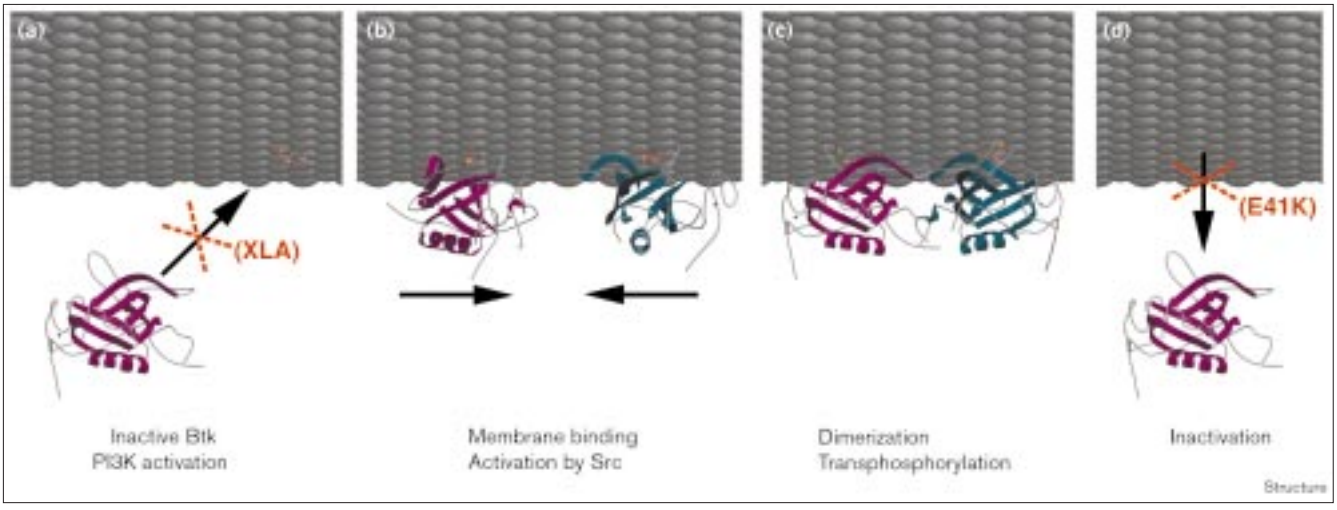


A model for the activation of Btk on the membrane. In the resting cells, Btk is cytosolic and inactive (**a**). Upon stimulation of the β-cell receptor, PI3K is activated and generates PtdIns(3,4,5)$P_3$. The Btk PH domain anchors the enzyme on the plasma membrane, where Btk is phosphorylated on Y551 in the activation loop of the kinase domain by Src (**b**). Btk dimerizes via lateral interactions between two PH domains (**c**). Dimeric Btk can trans-phosphorylate Y223 in the SH3 domain, resulting in a fully active enzyme. Btk is released from the membrane following dephosphorylation of PtdIns(3,4,5)P3 (**d**). The red crosses indicate steps where different PH mutations affect the normal activation pathway.

rapidly produced upon stimulation by the PI3K activity [52]. Consequently, PH domains that bind to these lipids have to interact with a much higher affinity and specificity in comparison with other domains because of the transient nature of the signal [36,37,42]. The structural studies described above reveal the details of this interaction in the case of the Btk PH domain. In particular, they show how the backbone of the β1–β2 loop that contacts the 5-phosphate of Ins(1,3,4,5)$P_4$ closes the binding site at one side, which probably accounts for the high affinity and specific binding. This binding mode might be common to the other PH domains known to bind specifically to PtdIns(3,4,5)$P_3$, such as the domains of GRP-1 and cytohesin (Figure 1b).

All three variant PH domains of Btk crystallized in an identical manner, as dimers with two molecules in the asymmetric unit, despite different space groups (Table 1 and [29]). Dimerization involves the same interface formed by the β1–β2 strands of the two monomers, where the sidechains of residues 41–45 in the β strand interact in an antiparallel mode. Using analytical ultracentrifugation and gel filtration we have not been able to detect dimers of the Btk domain in solution in the presence or absence of Ins(1,3,4,5)$P_4$. However, the dimer interface occupies a surface (~1100 $A^2$ per monomer) that is larger than the one normally found in nonspecific crystal contacts [53–55]. The decrease of solvent-accessible area caused by dimerization, as well as the number of hydrogen bonds stabilizing the dimer (nine), are comparable with the values observed for homodimers [56].

The dimerization tendency of the PH domains may have biological relevance for signalling. For its full activation, Btk undergoes autophosphorylation of the Y223 residue in the SH3 domain [13,14], but it is not yet clear whether this occurs via a *cis* or *trans* mechanism. The dimerization of PH domains could take place on the membrane surface. This can lead to the following model for the activation mechanism of Btk. First, PI3K is activated by B-cell receptor stimulation and generates the membrane-bound ligand, PtdIns(3,4,5)$P_3$. Second, Btk is recruited to the membrane via anchorage of its PH domain to PtdIns(3,4,5)$P_3$ and electrostatic interactions where it dimerizes as a result of the interaction of two PH domains. Third, the Y551 residue of Btk is phosphorylated by the Src kinase, and the Y223 residue is phosphorylated *in trans* by the Btk dimer. This completes the activation and generates stimuli for B-cell maturation. Finally, a phosphatase such as SHIP dephosphorylates PtdIns(3,4,5)$P_3$, leading to the release of Btk from the membrane and to its inactivation (Figure 8). In this model, the membrane would be an essential component for dimerization, limiting the Btk mobility to two dimensions, stabilizing this oligomeric state and regulating activation of the kinase. Dimerization of the Btk PH domain should be studied on lipid vesicles or lipid monolayers in order to test this model.

## Biological implications

Studies in this paper focus on the molecular basis of defects in the membrane association of Bruton's tyrosine kinase (Btk), which cause a human immunodeficiency called X-linked agammaglobulinemia. Btk is a key factor for the maturation of B cells. A variety of point mutations that result in a severe disease reside in the N-terminal PH (pleckstrin-homology) domain. This domain specifically binds phosphatidylinositol 3,4,5-trisphosphate, causing Btk to respond to signalling via phosphatidylinositol 3-kinase. The crystal structures of the wild-type PH domain and a mutant domain (E41K) in complex with D-*myo*-inositol 1,3,4,5-tetrakisphosphate show that the mutant phenotype has different causes. Some mutations simply perturb the stability of the PH domain or the adjacent Btk motif. Other mutant proteins are able to fold, but they display weakened binding of the phosphatidylinositol 3,4,5-trisphosphate head group in a specific binding site. Two mutations have an effect on the electrostatic potential in the region surrounding the phosphatidylinositol-binding site. The reversal of an electric charge in this region can cause a loss of function (K19E) or a gain of function (E41K). Finally, the Q127H mutation is predicted to perturb a different function, such as the interaction with a subunit of a trimeric G protein.

## Materials and methods

### *Crystallization and data collection*

Expression and purification of the PH domain from the wild-type Btk, and the mutants E41K, R28C, K19E, Q127H and T117P was carried out in *E. coli* strain BL21(DE3) as described previously [29]. A protein concentration of 10 mg/ml was used for crystallization. Proteins crystallized at room temperature in hanging drops. Mixing of the wild-type and E41K domain with the ligand D-Ins(1,3,4,5)$P_4$ was carried out immediately before setting the crystallization drops in a molar ratio of 1:4. The crystals of the E41K mutant grew with 10% (w/v) PEG 4000 (Sigma, USA), 100 mM Na acetate pH 5.5, whereas the wild type crystallized in 9% (w/v) PEG 4000, 100 mM Na acetate pH 4.9, 10% (v/v) methanol. In both cases, cubic crystals appeared after 12 hours. Each complex crystallized in the tetragonal space group $I4_122$ with cell dimensions a = b = 110.20 Å, c = 215.53 Å for the wild type, and a = b = 110.78 Å, c = 215.60 Å for the E41 mutant. Calculation of Matthews volume [57] gives $V_m$ = 4.12 $Å^3$/Da, assuming two molecules per asymmetric unit, which corresponds to 70.1% solvent content. 2-methyl-2,4-pentanediol was added to a final concentration of 20% (v/v) in the crystallization solution as a cryoprotectant during data collection. Diffraction data were collected at 100K using a Mar CCD detector on the ID14a beamline at ESRF synchrotron facility in Grenoble. The images were processed using the programs XDISPLAY, DENZO and SCALEPACK of the HKL package [58].

### *Structure determination and refinement*

The structure of the E41K mutant was solved by molecular replacement using the program AMoRe [59] and the single polypeptide chain of the refined R28C mutant structure [29] (PDB code 1btk) as a search model. The rotation search was carried out in the resolution range of 10.0–3.5 Å, with an outer radius of Patterson integration of 16.0 Å. The correct rotation solutions corresponded to peaks No. 1 (4.3σ) and No. 4 (3.4σ), as revealed by the translation function calculated with data in the 10.0–4.0 Å range. After rigid-body refinement, the R factor was 0.426, and the correlation coefficient was 0.549 for diffraction data between 20.0 and 3.5 Å. The initial model containing only the two polypeptide chains was refined with TNT [60], and the R factor dropped to 0.320 (15.0–2.1 Å). The $F_o$–$F_c$ map contoured at 3.0σ

clearly indicated positions of Ins(1,3,4,5)$P_4$ and the zinc ions, and the changed conformation of the β1–β2 loop in both molecules of the asymmetric unit. Ligands as well as zinc ions were included in the model and the β1–β2 loop was rebuilt. Several cycles of refinement of atomic positions and B factors with gradual release of noncrystallographic-symmetry (NCS) constraints were carried out, alternating with model-building sessions with the program O [61]. All diffraction data (35.0–2.1 Å) were used throughout refinement, apart from a randomly selected test set (6%) required for R-free calculations. Solvent positions were automatically assigned by peak-searching routines of TNT in combination with the WATPEAK program from the CCP4 suite [62], and they were also checked with the graphics program O for density and hydrogen-bonding patterns. Inspection of the difference $2F_o–F_c$ and $F_o–F_c$ maps (at R factor 0.221, R free 0.312) of the mutant domain showed the position of the second Ins(1,3,4,5)$P_4$ molecule in the proximity of residue K41 in each molecule within the asymmetric unit. The ligand, which is located on the crystallographic twofold axis with C2–C5 direction parallel to the symmetry element, was placed in the electron density and included in the model with occupancies set to 0.5, and refined thereafter as a rigid body. The refinement of positional and temperature parameters converged to an R factor of 0.214 and R free of 0.296 for diffraction data in the 35.0–2.1 Å resolution range. Residues 84–86 of molecule A, and 80–87 of molecule B were not clearly visible in electron-density maps and were not included in the model. In order to cross-check the orientation, the ligands were deleted from the model together with solvent molecules, and a random shift of 0.3 Å was applied to all atoms. The initial R factor of this model was 0.351 and it converged to 0.288 after 10 cycles of positional and temperature-factor refinement. The $2F_o–F_c$ and $F_o–F_c$ electron-density maps calculated with this model clearly correspond to the position and orientation of the ligand in the refined structure.

The wild-type Btk PH–Ins(1,3,4,5)$P_4$ complex crystallizes in the same crystal form as the E41K mutant, and the refined coordinates of the latter without the ligands, zinc ions and solvent molecules were used as the starting model. This was submitted to the rigid-body refinement, which reduced the R factor from 0.339 to 0.330 for the data between 35.0 and 4.0 Å. Subsequent positional and B-factor refinement with NCS restraints against data in the 35.0–2.4 Å resolution range reduced the R factor to 0.297. The location of Ins(1,3,4,5)$P_4$ in each subunit was clearly identified at this stage in the $2F_o–F_c$ and $F_o–F_c$ density maps. The ligand was built in the density, and the model was refined by several cycles of TNT with NCS restraints, combined with visual inspection of the model and water positions as located in the $F_o–F_c$ density maps. The refinement converged to an R factor of 0.234 and R free of 0.351 for diffraction data in the 35.0–2.4 Å resolution range. Residues 83–88 of molecule A and 80–86 of molecule B were not clearly visible in the electron density and were not included in the model. Details on data collection, refinement statistics and final model quality are given in Table 1.

### *Isothermal titration calorimetry*

All titration experiments were conducted using an MCS ITC system (Microcal Inc., MA) as described elsewhere [51,63]. Protein solutions were dialyzed against the buffer (10 mM TrisHCl pH 8.0, 100 mM NaCl, 2 mM DTT). The same buffer was used to dilute a concentrated stock solution of Ins(1,3,4,5)$P_4$. Titrations were performed at 15°C, in a series of 17 experiments, injecting, for each step, 15 μl of ligand (100 μM) into protein samples (10 μM) in the ITC cell (1.4 ml). Heats of dilution of ligand into buffer were determined with separate titrations and subtracted from the raw data of the binding experiments prior to analysis. Resulting data were fitted with least-squares regression using ORIGIN Software (Microcal) and a model for a single class of binding site, as indicated by the shape of the titrations [51]. Three parameters were allowed to float in the fitting procedure: change in enthalpy of interaction (ΔH), binding constant ($K_B = 1/K_D$) and stoichiometry. Values for the change in free energy (ΔG°) and entropy (ΔS°) for the interactions were calculated by

$$–RT \ln K_B = \Delta H – T\Delta S° = \Delta G°$$

where T is the absolute temperature and R is the gas constant. The data were close to the limits of detection of ITC and are therefore affected by large apparent errors in measurement.

### *Other methods*

D-Ins(1,3,4,5)$P_4$ was synthesized from *myo*-inositol as described previously [64] and was used as the 8 $K^+$ salt. $^{31}P$ and $^1H$ NMR spectra, mass spectra and optical rotation were all in accord with the final structure. The electrostatic potential for the Btk PH domains were calculated with the UHBD program [65], applying the finite difference Poisson–Boltzmann equation.

### *Accession numbers*

The structures of the wild-type and E41K complexes have been deposited in the Protein Data Bank [66] with accession codes 1b55 and 1bwn, respectively.

## Acknowledgements

We wish to thank W Burmeister and S Wakatsuki at ESRF-Grenoble for helping with the data collection, and Razif Gabdouilline for his help in the electrostatic-potential calculations. Work at Bath University was supported by a Wellcome Trust Programme Grant (045491) to BVLP.

## References

1. Bolen, J.B. (1993). Nonreceptor tyrosine protein kinases. *Oncogene* **8**, 2025-2031.
2. Saouaf, S.J., Burkhardt, A.L. & Bolen, J.B. (1995). Nonreceptor protein tyrosine kinase involvement in signal transduction and immunodeficiency disease. *Clin. Immunol. Immunopathol.* **76**, S151-157.
3. Tsukada, S., *et al*., & Witte, O.N. (1993). Deficient expression of a B cell cytoplasmic tyrosine kinase in human X-linked agammaglobulinemia. *Cell* **72**, 279-290.
4. Vetrie, D., *et al.*, & Bentley, D.R. (1993). The gene involved in X-linked agammaglobulinemia is a member of the src family of protein-tyrosine kinases. *Nature* **361**, 226-233.
5. Mattsson, P.T., Vihinen, M. & Smith, C.I.E. (1996). X-linked agammaglobulinemia (XLA): a genetic tyrosine kinase (Btk) disease. *Bioessays* **18**, 825-834.
6. Smith, C.I., *et al.*, & Hammarstrom, L. (1994). X-linked agammaglobulinemia and other immunoglobulin deficiencies. *Immunol. Rev.* **138**, 159-183.
7. Rawlings, D.J., *et al.*, & Kinet, J.P. (1996). Mutation of unique region of Bruton's tyrosine kinase in immunodeficient XID mice. *Science* **261**, 358-361.
8. Thomas, J.D., Sideras, P., Smith, C.I., Vorechovsky, I., Chapman, V. & Paul, W.E. (1993). Colocalization of X-linked agammaglobulinemia and X-linked immunodeficiency genes. *Science* **261**, 355-358.
9. Bolen, J.B (1995). Protein tyrosine kinases in the initiation of antigen receptor signaling. *Curr. Opin. Immunol.* **7**, 306-311.
10. Vihinen, M., Nilsson, L. & Smith, C.I.E. (1994). Tec homology (TH) adjacent to the PH domain. *FEBS Lett* **350**, 263-265.
11. Sato, S., *et al*., & Takatsu, K. (1994). IL-5 receptor-mediated tyrosine phosphorylation of SH2/SH3-containing proteins and activation of Bruton's tyrosine and Janus 2 kinases. *J. Exp. Med.* **180**, 2101-2111.
12. de Weers, M., *et al.*, & Borst, J. (1994). B-cell antigen receptor stimulation activates the human Bruton's tyrosine kinase, which is deficient in X-linked agammaglobulinemia. *J. Biol. Chem.* **269**, 23857-23860.
13. Rawlings, D.J., *et al.*, & Kinet, J.P. (1996). Activation of BTK by a phosphorylation mechanism initiated by SRC family kinases. *Science* **271**, 822-825.
14. Park, H., *et al*., & Witte, O.N. (1996). Regulation of Btk function by a major autophosphorylation site within the SH3 domain. *Immunity* **4**, 515-525.
15. Vihinen, M., *et al.*, & Smith, C.I.E. (1995). BTKbase: a database of XLA-causing mutations. International Study Group. *Immunol. Today* **16**, 460-465.
16. Scharenberg, A.M., *et al*., & Kinet, J.P. (1998). Phosphatidylinositol-3,4,5-trisphosphate (PtdIns-3,4,5-P3)/Tec kinase-dependent calcium signaling pathway: a target for SHIP-mediated inhibitory signals. *EMBO J.* **17**, 1961-1972.
17. Toker, A. & Cantley, L.C. (1997). Signalling through the lipid products of phosphoinositide-3-OH kinase. *Nature* **387**, 673-676.
18. Rameh, L.E., *et al.*, & Cantley, L.C. (1997). A comparative analysis of the phosphoinositide binding specificity of pleckstrin homology domains. *J. Biol. Chem.* **272**, 22059-22066.

19. Lioubin, M.N., Algate, P.A., Tsai, S., Carlberg, K., Aebersold, A. & Rohrschneider, L.R. (1996). p150Ship, a signal transduction molecule with inositol polyphosphate-5-phosphatase activity. *Genes Dev.* **10**, 1084-1095.
20. Damen, J.E., *et al*., & Krystal, G. (1996). The 145 kDa protein induced to associate with Shc by multiple cytokines is an inositol tetraphosphate and phosphatidyl-inositol 3,4,5-triphosphate 5-phosphatase. *Proc. Natl Acad. Sci. USA* **93**, 1689-1693.
21. Bolland, S., Pearse, R.N., Kurosaki, T. & Ravetch, J.V (1998). SHIP modulates immune receptor responses by regulating membrane association of Btk. *Immunity* **8**, 509-516.
22. Spiegel, S., Foster, D. & Kolesnick, R (1996). Signal transduction through lipid second messengers. *Curr. Opin. Cell Biol.* **8**, 159-167.
23. Takata, M. & Kurosaki, T (1996). A role for Bruton's tyrosine kinase in B cell antigen receptor-mediated activation of phospholipase C-γ2. *J. Exp. Med.* **184**, 31-40.
24. Fluckiger, A.C., *et al.*, & Rawlings, D.J. (1998). Btk/Tec kinases regulate sustained increases in intracellular $Ca^{2+}$ following B-cell receptor activation. *EMBO J.* **17**, 1973-1985.
25. Berridge, M.J. (1993). Inositol trisphosphate and calcium signalling. *Nature* **361**, 315-325.
26. Macias, M.J., Musacchio, A., Ponstingl, H., Nilges, M., Saraste, M. & Oschkinat, H. (1994). Structure of the pleckstrin homology domain from β-spectrin. *Nature* **369**, 675-677.
27. Yoon, H.S., Hajduk, P.J., Petros, A.M., Olejniczak, E.T., Meadows, R.P. & Fesik, S.W. (1994). Solution structure of a pleckstrin-homology domain. *Nature* **369**, 672-675.
28. Ferguson, K.M., Lemmon, M.A., Schlessinger, J. & Sigler, P.B. (1994). Crystal structure at 2.2 Å resolution of the pleckstrin homology domain from human dynamin. *Cell* **79**, 199-209.
29. Hyvönen, M. & Saraste, M. (1997). Structure of the PH domain and Btk motif from Bruton's tyrosine kinase: molecular explanations for X-linked agammaglobulinaemia. *EMBO J.* **16**, 3396-3404.
30. Blomberg, N. & Nilges, M.(1997). Functional diversity of PH domains: an exhaustive modelling study. *Fold. Des.* **2**, 343-355.
31. Ferguson, K.M., Lemmon, M.A., Schlessinger, J. & Sigler, P.B. (1995). Structure of the high affinity complex of inositol trisphosphate with a phospholipase C pleckstrin homology domain. *Cell* **83**, 1037-1046.
32. Harlan, J.E., Hajduk, P.J., Yoon, H.S. & Fesik, S.W. (1994). Pleckstrin homology domains bind to phosphatidylinositol-4,5- bisphosphate. *Nature* **371**, 168-170.
33. Salim, K., *et al*., & Panayotou, G. (1996). Distinct specificity in the recognition of phospho-inositides by the pleckstrin homology domains of dynamin and Bruton's tyrosine kinase. *EMBO J.* **15**, 6241-6250.
34. Lemmon, M.A., Ferguson, K.M., O'Brien, R., Sigler, P.B. & Schlessinger, J. (1995). Specific and high-affinity binding of inositol phosphates to an isolated pleckstrin homology domain. *Proc. Natl Acad. Sci. USA* **92**, 10472-10476.
35. Datta, K., Bellacosa, A., Chan, T.O. & Tsichlis, P.N. (1996). Akt is a direct target of the phosphatidylinositol 3-kinase. Activation by growth factors, v-src and v-Ha-ras, in Sf9 and mammalian cells. *J. Biol. Chem.* **271**, 30835-30839.
36. Frech, M., Andjelkovic, M., Ingley, E., Reddy, K.K., Falck, J.R. & Hemmings, B.A. (1997). High affinity binding of inositol phosphates and phosphoinositides to the pleckstrin homology domain of RAC/protein kinase B and their influence on kinase activity. *J. Biol. Chem.* **272**, 8474-8481.
37. Klarlund, J.K., Guilherme, A., Holik, J.J., Virbasius, J.V., Chawla, A. & Czech, M.P. (1997). Signaling by phosphoinositide-3,4,5-trisphosphate through proteins containing pleckstrin and Sec7 homology domains. *Science* **275**, 1927-1930.
38. Hyvönen, M., Macias, M.J., Nilges, M., Oschkinat, H., Saraste, M. & Wilmanns, M. (1995). Structure of the binding site for inositol phosphates in a PH domain. *EMBO J.* **14**, 4676-4685.
39. Fukuda, M., Kojima, T., Kabayama, H. & Mikoshiba, K. (1996). Mutation of the pleckstrin homology domain of Bruton's tyrosine kinase in immuno-deficiency impaired inositol 1,3,4,5-tetrakisphosphate binding capacity. *J. Biol. Chem.* **271**, 30303-30306.
40. Li, T., *et al*., & Witte, O.N. (1995). Activation of Bruton's tyrosine kinase (BTK) by a point mutation in its pleckstrin homology (PH) domain. *Immunity* **2**, 451-460.
41. Li, T., Rawlings, D.J., Park, H., Kato, R.M., Witte, O.N. & Satterthwaite, A.B. (1997). Constitutive membrane association potentiates activation of Bruton's tyrosine kinase. *Oncogene* **15**, 1375-1383.
42. Kojima, T., Fukuda, M., Watanabe, Y., Hamazato, F. & Mikoshiba, K.(1997). Characterization of the pleckstrin homology domain of Btk as an inositol polyphosphate and phosphoinositide binding domain. *Biochem. Biophys. Res. Commun.* **236**, 333-339.
43. Downing, A.K., Driscoll, P.C., Gout, I., Salim, K., Zvelebil, M.J. & Waterfield, M.D. (1994). Three-dimensional solution structure of the pleckstrin homology domain from dynamin. *Curr. Biol.* **4**, 884-891.
44. Fushman, D., Cahill, S., Lemmon, M.A., Schlessinger, J. & Cowburn, D. (1995). Solution structure of pleckstrin homology domain of dynamin by heteronuclear NMR spectroscopy. *Proc. Natl Acad. Sci. USA* **92**, 816-820.
45. Koshiba, S., Kigawa, T., Kim, J.H., Shirouzu, M., Bowtell, D. & Yokoyama, S. (1997). The solution structure of the pleckstrin homology domain of mouse Son-of-sevenless 1 (mSos1). *J. Mol. Biol.* **269**, 579-591.
46. Timm, D., Salim, K., Gout, I., Guruprasad, L., Waterfield, M. & Blundell, T. (1994). Crystal structure of the pleckstrin homology domain from dynamin. *Nat. Struct. Biol.* **1**, 782-788.
47. Koch, W.J., Inglese, J., Stone, W.C. & Lefkowitz, R.J. (1993). The binding site for the beta gamma subunits of heterotrimeric G proteins on the beta-adrenergic receptor kinase. *J. Biol. Chem.* **268**, 8256-8260.
48. Tsukada, S., Simon, M.I., Witte, O.N. & Katz, A. (1994). Binding of beta gamma subunits of heterotrimeric G proteins to the PH domain of Bruton tyrosine kinase. *Proc. Natl Acad. Sci. USA* **91**, 11256-11260.
49. Bence, K., Ma, W., Kozasa, T. & Huang, X.-Y. (1997). Direct stimulation of Bruton's tyrosine kinase by G(q)-protein alpha-subunit. *Nature* **389**, 296-299.
50. Jiang, Y., Ma, W., Wan, Y., Kozasa, T., Hattori, S. & Huang, X.-Y (1998). The G protein Ga12 stimulates Bruton's tyrosine kinase and a rasGAP through a conserved PH/BM domain. *Nature* **395**, 808-813.
51. Wiseman, T., Williston, S., Brandts, J.F. & Lin, L.N. (1989). Rapid measurement of binding constants and heats of binding using a new titration calorimeter. *Anal. Biochem.* **179**, 131-137.
52. Carpenter, C.L. & Cantley, L.C. (1996). Phosphoinositide kinases. *Curr. Opin. Cell Biol.* **8**, 153-158.
53. Janin, J. & Rodier, F. (1995). Protein-protein interaction at crystal contacts. *Proteins* **23**, 580-587.
54. Carugo, O. & Argos, P. (1997) Protein-protein crystal-packing contacts. *Protein Sci.* **6**, 2261-2263.
55. Janin, J. (1997). Specific versus non-specific contacts in protein crystals. *Nat. Struct. Biol.* **4**, 973-974.
56. Jones, S. & Thornton, J.M. (1996). Principles of protein-protein interactions. *Proc. Natl Acad. Sci. USA* **93**, 13-20.
57. Matthews, B.W. (1968). Solvent content of protein crystals. *J. Mol. Biol.* **33**, 491-497.
58. Otwinowski, Z. (1997). Processing of X-ray diffraction data collected in oscillation mode. *Methods enzymol.* **276**, 307-326.
59. Navazza, J. (1994) AMoRe: an automated package for molecular replacement. *Acta Crystallogr. A* **50**, 157-163.
60. Tronrud, D.E. (1992) Conjugate gradient minimization: an improved method for the refinement of macromolecules. *Acta Crystallogr. A* **48**, 912-916.
61. Jones, T.A., Cowan, S., Zou, J.-Y. & Kjeldgaard, M. (1991). Improved methods for building protein models in electron density maps and the location of errors in these models. *Acta Crystallogr. A* **47**, 110-119.
62. Collaborative Computational Project, Number 4. (1994). The CCP4 Suite: programs for protein crystallography. *Acta Crystallogr. D* **50**, 760-763.
63. Ladbury, J.E. & Chowdhry, B.Z. (1996). Sensing the heat: the application of isothermal titration calorimetry to thermodynamic studies of biomolecular interactions. *Chem. Biol.* **3**, 791-801.
64. Riley, A.M., Mahon, M.F. & Potter, B.V.L. (1997). Rapid synthesis of the enantiomers of *myo*-inositol-1,3,4,5-tetrakisphosphate by direct chiral desymmetrization of *myo*-inositol orthoformate. *Angew. Chem. Int. Edn Eng.* **36**, 1472-1474.
65. Madura, J.D., *et al*., & McCammon, J.A. (1995). Electrostatic and diffusion of molecules in solution: simulations with the University of Houston Brownian Dynamics Program. *Comp. Phys. Commun.* **91**, 57-95.
66. Bernstein, F.C., *et al.*, & Tasumi, M. (1977). The protein data bank: a computer-based archival file for macromolecular structures. *J. Mol. Biol.* **112**, 535-542.
67. Cohen, G.E. (1997). ALIGN: A program to superimpose protein coordinates, accounting for insertions and deletions. *J. Appl. Crystallogr.* **30**, 1160-1161.
68. Evans, S.V. (1993). SETOR: hardware lighted three-dimensional solid model representations of macromolecules. *J. Mol. Graph.* **11**, 134-138.
69. Wallace, A.C., Laskowski, R.A. & Thornton, J.M. (1995). LIGPLOT: A program to generate schematic diagrams of protein-ligand interactions. *Prot. Eng.* **8**, 127-134.
70. Insight II User Guide, September 1995. San Diego: Biosym/MSI.
71. Vihinen, M., *et al*., & Smith, C.I.E. (1998). BTKbase, mutation database for X-linked agammaglobulinemia (XLA). *Nucleic Acids Res.* **26**, 242-247.